

Zeitschrift: Helvetica Physica Acta
Band: 46 (1973)
Heft: 5

Artikel: Entropy of a type-II superconductor close to the critical temperature
Autor: Ehrat, R. / Rinderer, L.
DOI: <https://doi.org/10.5169/seals-114504>

Nutzungsbedingungen

Die ETH-Bibliothek ist die Anbieterin der digitalisierten Zeitschriften auf E-Periodica. Sie besitzt keine Urheberrechte an den Zeitschriften und ist nicht verantwortlich für deren Inhalte. Die Rechte liegen in der Regel bei den Herausgebern beziehungsweise den externen Rechteinhabern. Das Veröffentlichen von Bildern in Print- und Online-Publikationen sowie auf Social Media-Kanälen oder Webseiten ist nur mit vorheriger Genehmigung der Rechteinhaber erlaubt. [Mehr erfahren](#)

Conditions d'utilisation

L'ETH Library est le fournisseur des revues numérisées. Elle ne détient aucun droit d'auteur sur les revues et n'est pas responsable de leur contenu. En règle générale, les droits sont détenus par les éditeurs ou les détenteurs de droits externes. La reproduction d'images dans des publications imprimées ou en ligne ainsi que sur des canaux de médias sociaux ou des sites web n'est autorisée qu'avec l'accord préalable des détenteurs des droits. [En savoir plus](#)

Terms of use

The ETH Library is the provider of the digitised journals. It does not own any copyrights to the journals and is not responsible for their content. The rights usually lie with the publishers or the external rights holders. Publishing images in print and online publications, as well as on social media channels or websites, is only permitted with the prior consent of the rights holders. [Find out more](#)

Download PDF: 27.01.2026

ETH-Bibliothek Zürich, E-Periodica, <https://www.e-periodica.ch>

Entropy of a Type-II Superconductor Close to the Critical Temperature

by R. Ehrat¹⁾ and L. Rinderer

Institut de Physique Expérimentale de l'Université de Lausanne, Lausanne, Switzerland

(27. VI. 73)

Abstract. The experimental values for the incremental entropy, $S_i = \phi_0(\partial S/\partial B)|_T$, of vortices in the mixed state, have been determined for the alloy Nb80Mo20 ($K \approx 4$). From specific heat data for $C_s(T)$ in the superconducting state and $C_n(T)$ in the normal state, this alloy is shown to behave as a BCS superconductor. The results for $S_i(B)$ are compared with theoretical values deduced from the Abrikosov free energy at high fields, extended to arbitrary temperatures, and from the London energy at low fields. Integrating $S_i(B)$, the experimental entropy curves at constant induction, $S(T)|_B$, can be constructed and experimental values for C_B , the specific heat at constant induction, are indirectly obtained from graphical differentiation. At the mixed-normal phase transition and close to T_c , the results suggest that C_B is continuous and tends to $C_s(T_c)$, in contradiction to the theoretical predictions. This is in thermodynamic agreement with anomalous results for C_H already obtained on the same sample. The consequences of this new information are analysed.

I. Introduction

The equilibrium free energy per unit volume F , for a bulk superconductor of the second kind, is a function of temperature T and magnetic induction B . All calculations for F in the mixed state are based on extensions to low temperatures of the Ginzburg–Landau–Abrikosov–Gorkov theory [1–3] (GLAG), which is valid only close to the critical temperature T_c . These calculations try to cover the whole mixed state, from the first penetration field H_{c1} to the upper critical field H_{c2} [4].

According to calculations within the frame of the GLAG theory, both phase transitions at H_{c1} and H_{c2} are second order [5] for all values of the GL parameter K larger than the critical value $K_{cr} = 1/\sqrt{2}$ (type II). The initial penetration of flux occurs under the form of isolated vortices carrying one flux quantum ϕ_0 . The second-order nature [6, 7] of the transition at H_{c1} is a consequence of the repulsive interaction between vortices [8–10]. However, since this interaction is short range [11], an infinite slope of the magnetization curve is predicted at H_{c1} (λ transition), while the magnetization M decreases linearly to zero close to H_{c2} where the slope shows a finite discontinuity. If a number of theoretical and experimental works [5] tend to establish the existence at low temperatures of a first-order transition (finite discontinuity of M) at H_{c1} , in critical K type-II superconductors ($K \lesssim 1/\sqrt{2}$), it is however admitted that the attractive interaction implied by such a transition is negligible for T close to T_c , where the conclusions of the GLAG theory ought to be strictly valid. Concerning superconductors

¹⁾ Present address: Zentralinstitut für Tieftemperaturforschung der Bayerischen Akademie der Wissenschaften, Garching, Germany.

with $K \gg 1/\sqrt{2}$, the transition at H_{c1} ought probably to be second order for any temperature [12].

Because of experimental difficulties, magnetization measurements are usually performed for temperatures significantly smaller than T_c only. As extrapolations of the experimental results to T_c are in good agreement with theoretical predictions [13], there have been no reasons to doubt the validity of the Abrikosov solution of GL equations for bulk samples (diameter $\lesssim 1$ mm). Indeed, although this solution is valid for an infinite and homogeneous medium, a size effect should be expected for such specimens within a temperature range of the order of 10^{-8} °K of T_c . If the metallurgical quality of the samples would allow such a size effect to be observed, a detailed study within such a small temperature range would anyhow remain out of actual experimental possibilities.

However, our calorimetric measurements on a Nb80Mo20 sample, in fields much smaller than those used by other authors, have shown near H_{c2} and close to T_c a continuous behaviour of C_H , the specific heat in a constant magnetic field, instead of the discontinuous behaviour predicted by the theory [14]. This anomaly, in respect to the theoretical predictions, occurred for fields smaller than 100 Oe or $t = T/T > 0.98$. A detailed analysis showed that trivial explanations involving effects in connection with non-perfect, 'real' samples could be apparently excluded. Two points could be examined:

- i) Such an effect could be eventually observed on other type-II superconductors. A partial answer could be given on a Pb98In2 alloy [14], suggesting further experiments.
- ii) From thermodynamic considerations, an anomaly of C_H should be related to anomalies of other magnetic or thermal quantities. Measurements on the same sample (Nb80Mo20) of the incremental entropy of vortices, S_i , ought to give an experimental answer to this question. Such results are analysed in this paper.

Unfortunately, experimental values of M and S_i are not reliable very close to T_c for reasons which will be discussed in Section III. This is the reason why extrapolated values of C_B , the specific heat at constant induction B , will be indirectly determined from S_i measurements at lower temperatures. More generally, the experimental entropy behaviour will be studied for all fields near T_c , and compared with theoretical predictions.

II. Theoretical Values for the Free Energy in the Mixed State

1. Definitions and thermodynamic relations

When the external magnetic field is increased from zero up to H_{c2} , F increases from the pure superconducting value, $F_s(T, 0)$, in the Meissner state, up to the following normal state value:

$$F(T, H_{c2}) = F_s(T, 0) + \frac{H_c^2(T)}{8\pi} + \frac{H_{c2}^2(T)}{8\pi}. \quad (1)$$

$H_c^2/8\pi$ is the condensation energy for the temperature T and $H_{c2}^2/8\pi$ is the field energy in the normal state. The paramagnetism or diamagnetism of the normal state, as well as the kinetic energy of surface supercurrents (finite samples), are neglected.

The thermodynamic critical field H_c is defined by the well-known relation:

$$F_n(T, 0) - F_s(T, 0) = \frac{H_c^2(T)}{8\pi}. \quad (2)$$

The Gibbs energy is introduced by the Legendre transformation: $G(T, H) = F(T, B) - (BH/4\pi)$. For fixed H and T , the equilibrium value of B is obtained from the constitutive relation (equation of states) between the three coordinates (T, H, B) : $H = 4\pi(\partial F/\partial B)|_T$. The entropy S and the induction B are first derivatives of energy defined by the relations

$$\begin{aligned} dF &= -S dT + \frac{1}{4\pi} H dB \\ dG &= -S dT - \frac{1}{4\pi} B dH. \end{aligned} \quad (3)$$

M is related to B by $B = H + 4\pi M$ (zero demagnetizing factor). S can always take the form

$$S(T, B) = S_s(T) + \Delta S(T, B),$$

S_s being the entropy in the pure superconducting state. ΔS is always positive in the mixed state. We can alternatively write a $\Delta S(T, H)$ function using the constitutive relation. We consider the three thermal quantities

$$\begin{aligned} C_H &= T \frac{\partial S}{\partial T} \bigg|_H = C_s(T) + T \frac{\partial(\Delta S)}{\partial T} \bigg|_H \\ C_B &= T \frac{\partial S}{\partial T} \bigg|_B = C_s(T) + T \frac{\partial(\Delta S)}{\partial T} \bigg|_B \\ S_i &= \phi_0 \frac{\partial S}{\partial B} \bigg|_T = \phi_0 \frac{\partial(\Delta S)}{\partial B} \bigg|_T. \end{aligned} \quad (4)$$

C_H and S_i are directly measurable quantities. It can be easily shown that the following thermodynamic relations hold,

$$C_H - C_B = T \frac{S_i}{\phi_0} \frac{\partial(4\pi M)}{\partial T} \bigg|_H, \quad (5)$$

or, alternatively, using the Maxwell relation,

$$\begin{aligned} \frac{\partial B}{\partial T} \bigg|_H &= 4\pi \frac{\partial S}{\partial H} \bigg|_T \\ \frac{\partial(\Delta S)}{\partial T} \bigg|_H - \frac{\partial(\Delta S)}{\partial T} \bigg|_B &= 4\pi \left[\frac{\partial(\Delta S)}{\partial B} \bigg|_T \right]^2 \cdot \frac{\partial B}{\partial H} \bigg|_T. \end{aligned} \quad (6)$$

The second member of (6) is essentially positive or zero in the whole mixed state. This will be of importance in discussing limiting experimental values, at T_c , for C_B and C_H .

2. Free energy in the mixed state

A general expression for F cannot be given for all T and B [11, 4]. We must consider successively the region close to H_{c2} , the region close to H_{c1} and the intermediate region.

a) $B \approx H_{c2}$

For any temperature and any impurity concentration, the extended GLAG theory yields [4]:

$$G(H, T) - G_n(H, T) = -\frac{1}{8\pi} \left\{ \frac{[\sqrt{2}K_1(T)H_c(T) - H]^2}{\beta[2K_2^2(T) - \eta(T, K)]} \right\}. \quad (7)$$

K_1 and K_2 are the temperature-dependent Maki parameters defined by the relations

$$\begin{aligned} K_1(T) &= H_{c2}(T)/\sqrt{2}H_c(T) \\ 4\pi \frac{\partial M}{\partial H} \bigg|_T &= (H_{c2}) = [\beta(2K_2^2 - 1)]^{-1}. \end{aligned} \quad (8)$$

They both are equal to K (GL) at T_c . For high temperatures and $K \gg 1$, we get for the parameter $\eta(T)$ introduced by Eilenberger [15]: $\eta(T) \approx 1$. The triangular structure, with $\beta = 1.1596$, is probably the most stable structure at any temperature. If we define $\gamma_2(T)$ as

$$\gamma_2(T) = 1 + \beta[2K_2^2(T) - 1], \quad (9)$$

the thermodynamic potentials and the constitutive relation take the following form:

$$\left. \begin{aligned} F &= F_n(T, 0) + \frac{1}{8\pi} [B^2 - \gamma_2^{-1}(H_{c2} - B)^2] \\ G &= G_n(T, 0) - \frac{1}{8\pi} [H^2 + (\gamma_2 - 1)^{-1} (H_{c2} - H)^2] \end{aligned} \right\} \quad (10)$$

$$B = H - (\gamma_2 - 1)^{-1}(H_{c2} - H). \quad (11)$$

Calculating the entropy (γ' is $d\gamma/dT$), one obtains:

$$\left. \begin{aligned} S(T, B) &= S_n(T, 0) + \frac{1}{4\pi\gamma_2} (H_{c2} - B) \left[H'_{c2} - \frac{\gamma'_2}{2\gamma_2} (H_{c2} - B) \right] \\ S(T, H) &= S_n(T, 0) + \frac{1}{4\pi(\gamma_2 - 1)} (H_{c2} - H) \left[H'_{c2} - \frac{\gamma'_2}{2(\gamma_2 - 1)} (H_{c2} - H) \right] \end{aligned} \right\}, \quad (12)$$

we then obtain the thermal quantities defined by (4),

$$\left. \begin{aligned} S_i &= -\frac{\phi_0}{4\pi\gamma_2} \frac{dH_{c2}}{dT} + \frac{\phi_0}{4\pi} \frac{\gamma'_2}{\gamma_2^2} (H_{c2} - B) \\ C_B - C_n &= \frac{T}{4\pi\gamma_2} \left(\frac{dH_{c2}}{dT} \right)^2 + \frac{T}{4\pi\gamma_2} (H_{c2} - B) \cdot \Phi_B \\ C_H - C_n &= \frac{T}{4\pi(\gamma_2 - 1)} \left(\frac{dH_{c2}}{dT} \right)^2 + \frac{T}{4\pi(\gamma_2 - 1)} (H_{c2} - H) \cdot \Phi_H \end{aligned} \right\} \quad (13)$$

Φ_B and Φ_H are functions of H_{c2} , H'_{c2} , H''_{c2} , γ_2 , γ'_2 , γ''_2 and B (or H). The relations (13) are valid for all K values ($K > 1/\sqrt{2}$). At the mixed-normal phase transition ($B \approx H \approx H_{c2}$), all terms on the right are zero except the first ones. It can be verified, taking account of (11), that these simplified relations satisfy the thermodynamic relation (5). The entropy is continuous at the transition, while C_H , C_B and S_i are discontinuous (S_i is zero in the normal state), in agreement with the assumption of a second-order phase transition.

b) $B \approx 0$ ($d > \lambda$)

For $K \gg 1$, F may be calculated by means of the 'London model'. If the lattice parameter, $d = (2\phi_0/\sqrt{3}B)^{1/2}$, is larger than the penetration depth, λ , we get

$$F_L = F_s + \frac{B}{4\pi} \left[H_{c1}(T) + \frac{3\phi_0}{2\pi\lambda^2(T)} K_0 \left(\frac{d}{\lambda(T)} \right) \right]. \quad (14)$$

The last term describes the repulsive interaction energy between fluxoids, where the six nearest neighbours only (triangular case) are considered for the calculation. K_0 is the zero-order Bessel function defined by the equation [16]

$$x^2 \frac{d^2 K_0}{dx^2} + x \frac{dK_0}{dx} - x^2 K_0 = 0 \quad (x = d/\lambda). \quad (15)$$

Taking into account the definition of K_0 , we obtain after two differentiations

$$S_i = -\frac{\phi_0}{4\pi} \left[\frac{dH_{c1}}{dT} + \frac{3\phi_0}{2\pi\lambda^3} \frac{d\lambda}{dT} \left(\frac{x^2}{2} - 2 \right) K_0(x) \right]. \quad (16)$$

For infinitely large d values, K_0 tends to zero. The result,

$$S_i(B=0) = -\frac{\phi_0}{4\pi} \frac{dH_{c1}}{dT},$$

was already obtained by Stephen [17].

c) *Intermediate region ($\lambda \gg d \gg \xi$)*

When the density, $n_L = B/\phi_0$, of fluxoids increases, the interactions extend to distant neighbours. So far as d remains much larger than the coherence length, ξ , the following expression, F_L^e , holds for the extended London free energy [11]:

$$F_L^e = F_s + \frac{B}{4\pi} \left[\frac{B}{2} + H_{c1} \frac{\ln \alpha(d/\xi)}{\ln(\lambda/\xi)} \right]. \quad (17)$$

The constant, $\alpha = 0.381$, is characteristic of the triangular lattice. From a straightforward calculation, we get:

$$\left. \begin{aligned} S_i &= -\frac{\phi_0}{4\pi} \cdot \frac{d\varphi}{dT} \left[\ln \left(\alpha \frac{d}{\xi} \right) + \psi(T) \right] \\ \varphi &= H_{c1} \left(\ln \frac{\lambda}{\xi} \right)^{-1}, \quad \psi = -\frac{1}{2} - \frac{\varphi \xi'}{\varphi' \xi} (\approx 0, 1). \end{aligned} \right\} \quad (18)$$

It was already mentioned [18] that the relation (17) ought to be applied only in the case of K values larger than 10.

3. Limiting values of C_B , C_H and S_i , in the mixed state, for $B \approx H_{c2}$ and $T \approx T_c$

We compute the limit, at the mixed-normal state transition and as T goes to T_c , for the theoretical values (13) as function of H_c and K . Close to T_c , we get

$$K = K_2(T_c) = K_1(T_c) = \lim_{T \rightarrow T_c} H_{c2}(T) / \sqrt{2} H_c(T).$$

Consequently,

$$\lim_{T \rightarrow T_c} \left(\frac{dH_{c2}}{dT} \right) = \sqrt{2} K \left(\frac{dH_c}{dT} \right)_{T_c} \quad \text{since } H_c(T_c) = 0.$$

Thus

$$\left. \begin{aligned} S_i(T \approx T_c) &= -\frac{\phi_0 \sqrt{2} K}{4\pi\gamma} \left(\frac{dH_c}{dT} \right)_{T_c} T_c \\ [C_B - C_n]_{T \approx T_c} &= \frac{T_c}{4\pi} \cdot \frac{2K^2}{\gamma} \cdot \left(\frac{dH_c}{dT} \right)_{T_c}^2 \\ [C_H - C_n]_{T \approx T_c} &= \frac{T_c}{4\pi} \cdot \frac{2K^2}{\gamma-1} \left(\frac{dH_c}{dT} \right)_{T_c}^2. \end{aligned} \right\} \quad (19)$$

For $H = 0$, the well-known thermodynamic Rutgers [19] relation holds:

$$\Delta C_R = [C_s - C_n]_{T=T_c} = \frac{T_c}{4\pi} \left(\frac{dH_c}{dT} \right)_{T_c}^2. \quad (20)$$

To compare the limiting values for C_B and C_H (19), as B or H goes to zero, with the value of C_s in zero field (20), we compute the ratios:

$$\left. \begin{aligned} \beta_B^* &= \lim_{B \approx H_{c2} \rightarrow 0} \left[\frac{\Delta C_R}{T_c} \right] \left(\frac{C_B - C_n}{T} \right) = \frac{\gamma}{2K^2} = \beta - \frac{\beta-1}{2K^2} \\ \beta_H^* &= \lim_{H \approx H_{c2} \rightarrow 0} \left[\frac{\Delta C_R}{T_c} \right] \left(\frac{C_H - C_n}{T} \right) = \frac{\gamma-1}{2K^2} = \beta \left(1 - \frac{1}{2K^2} \right). \end{aligned} \right\} \quad (21)$$

The theoretical β_B^* and β_H^* depend on K , and are different from unity in general, involving a discontinuous behaviour of C_B and C_H at T_c . The slopes of entropy curves for B (or H) = const. can be also calculated, at $T = T_c$, using (4), (20) and (21):

$$\left. \begin{aligned} \lim_{B \approx H_{c2} \rightarrow 0} \frac{\partial(\Delta S)}{\partial T} \Big|_B &= \frac{1}{4\pi} \left(\frac{dH_c}{dT} \right)_{T_c}^2 \left(\frac{1}{\beta_B^*} - 1 \right) \\ \lim_{H \approx H_{c2} \rightarrow 0} \frac{\partial(\Delta S)}{\partial T} \Big|_H &= \frac{1}{4\pi} \left(\frac{dH_c}{dT} \right)_{T_c}^2 \left(\frac{1}{\beta_H^*} - 1 \right). \end{aligned} \right\} \quad (22)$$

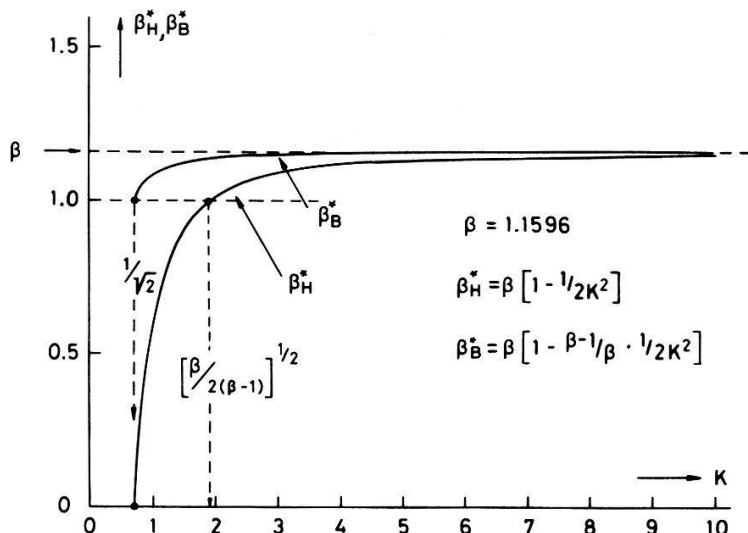


Figure 1

Values for the ratios β_B^* and β_H^* defined by the relations (21), and calculated according to the GLAG theory as functions of the GL parameter K .

The theoretical curves $\beta_B^*(K)$ and $\beta_H^*(K)$ are drawn in Figure 1. For any $K > 1/\sqrt{2}$, we get the result $\beta_B^* > 1$, which leads to the following inequalities:

$$\lim C_B < C_s(T_c) \quad \text{and} \quad \lim \left. \frac{\partial(\Delta S)}{\partial T} \right|_B < 0.$$

On the other hand we remark that

$$\lim C_H > C_s(T_c) \quad \text{and} \quad \lim \left. \frac{\partial(\Delta S)}{\partial T} \right|_H > 0 \quad \text{for } K < \sqrt{\frac{\beta}{2(\beta-1)}} \approx 1.9.$$

Our measurements of C_H on a Nb80Mo20 ($K \approx 4 > 1.9$) sample have shown a continuous behaviour close to T_c (β_H^* experimental ≈ 1), which is in contradiction with the theory [14]. We analyse here the entropy curves at constant induction $\Delta S(T)|_B$ in the whole mixed state, close to T_c , and try to extrapolate an experimental value for β_B^* .

III. Relation Between the Spatial Distribution of Impurities in a Superconductor and the Thermal Behaviour at a Phase Transition

All theoretical relations which have been established in the preceding section are valid for an infinite and homogeneous medium. 'Real' samples, of course, do not satisfy these requirements and present disturbing effects for values of T and H close to the critical values, which may make the comparison with theory difficult. For example, S_i values show a broad and continuous decrease close to H_{c2} instead of the expected sharp discontinuity. It is shown that in the case of the rather 'dirty superconductor'

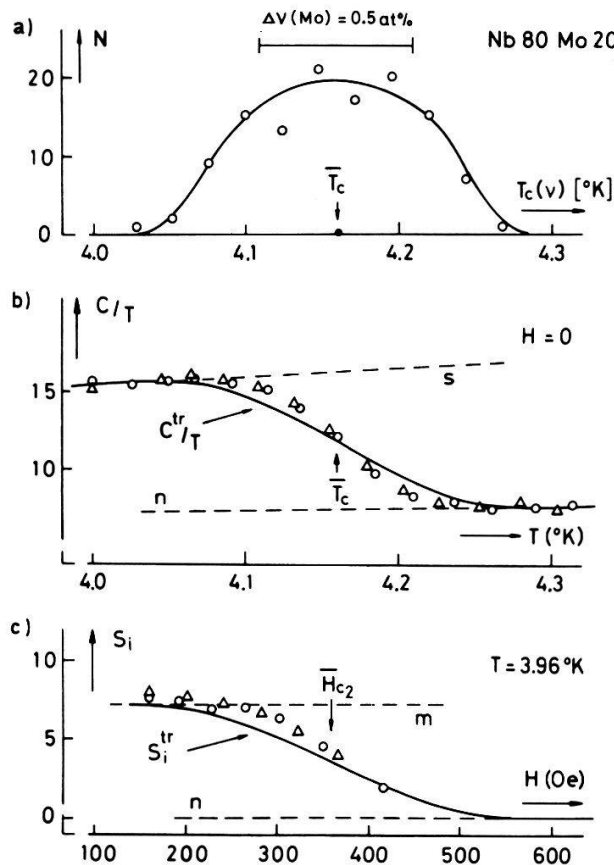


Figure 2

Distribution function N of molybdenum concentration ν inside the sample, determined by means of an electron microprobe x-ray analyser (2a). The knowledge of $N(\nu)$ and $T_c(\nu)$ allows one to calculate the real transition curves, $C^{tr}(T)$ and $S_i^{tr}(H)$, for the specific heat (2b) and the incremental entropy of vortices (2c).

studied here, such an effect is qualitatively and quantitatively explained by spatial fluctuations of the impurity concentration inside the sample.

Data have already been given concerning the geometrical and metallurgical properties of the cylindrical Nb80Mo20 sample studied here [14]. Two pieces were cut from the ends for electron microprobe X-ray analysis. From more detailed analysis than previously reported [14], the concentration ν of molybdenum was measured at 140 places scaled on seven different diameters. The mean value of these measurements, $\bar{\nu}$, corresponded to the critical temperature $\bar{T}_c = T_c = 4.16$ °K, determined from H_c measurements [14]. From $T_c(\nu)$ values reported by French and Lowell [20], a value for the slope, $dT_c/d\nu$ (20 at. % Mo) ≈ 0.2 °K/at. %, has been obtained which allowed us to estimate the T_c values, inside the sample as ranging between 4.03 °K and 4.28 °K.

On dividing this range in intervals of equal magnitude, $\Delta\nu = 0.12$ at. % ($\Delta T_c = 0.024^\circ\text{K}$), and on counting the number of observations falling inside each interval, a kind of gaussian distribution function $N(\nu)$, or $N(T_c)$, is obtained (Fig. 2a). Smaller intervals cannot be chosen without increasing the total number of measurements, or else the number of results falling inside a single interval is too small to get reliable statistical information. For a given T , we denote by $\alpha(T)$ the ratio of the volume of domains in which $T_c < T$, to the total volume of the sample. Integrating $N(T_c)$, we get:

$$\alpha(T) = \frac{\int_0^T N(T_c) dT_c}{\int_0^{+\infty} N(T_c) dT_c}.$$

The transition curve for the specific heat in zero field, C^{tr} , may be calculated knowing the values of $C_n(T)$ and $C_s(T)$ in the normal and superconducting states (Fig. 2b, n and s curves). Applying a superposition principle, we get:

$$C^{\text{tr}}(T) = \alpha C_n(T) + (1 - \alpha) C_s(T).$$

Good agreement is observed between the calorimetric values and the so-calculated 'metallurgical' curve. Calorimetric points have been denoted by circles if obtained with increasing temperature or field, and by triangles in the opposite case.

Such a calculation explains also the behaviour of S_i close to the transition to the normal state (Fig. 2c). The curves $H_{c2}(T, \nu)$ are easily deduced noting that, near T_c , the slope dH_{c2}/dT does not appreciably depend on T and ν . Thus we can write:

$$H_{c2}(T, \nu) = \left(\frac{dH_{c2}}{dT} \right)_{T_c} [T - T_c(\nu)].$$

On such a curve, the value of α is constant and equal to $\alpha[T_c(\nu)]$. For a given T , $\alpha(T, H)$ is obtained by looking for the $H_{c2}(T, \nu)$ curve through the point (T, H) , and we get, since S_i is zero in the normal state, $S_i^{\text{tr}}(T, H) = [1 - \alpha(T, H)] S_i^m$. Similar good agreement is observed in Figure 2c as in Figure 2b. \bar{H}_{c2} is of course defined by the relation,

$$\bar{H}_{c2} = H_{c2}(T, \bar{\nu}).$$

In conclusion, these results show that, even in the presence of a magnetic field, the total thermal behaviour observed at the transition is the sum of individual thermal behaviours of single ν domains. There are good reasons to explain the slight discrepancy between the calculated and measured transition curves by systematic errors in our determination of $N(T_c)$. The best experimental approximation for the value of S_i at H_{c2} , which would correspond to the ideal case of the homogeneous sample with concentration $\bar{\nu}$, is obtained by measuring the vertical distance between the two extrapolated curves, m and n , at \bar{H}_{c2} . Experimental points belonging to the S_i^{tr} curve ($\alpha > 0$) must be, of course, excluded for the determination of the m curve. Consequently, direct comparison of experimental and theoretical values for S_i close to H_{c2} does not make sense for fields smaller than ~ 200 Oe (see Section V). On the other hand, the analysis of C_H had been possible down to fields of the order of ~ 20 Oe.

IV. The Normal and Superconducting States of the Alloy Nb80Mo20

From specific heat measurements in zero and above-critical magnetic fields, the experimental values for $C_s(T)$ and $C_n(T)$ are obtained (see Fig. 3). Suitable integrations of these data yield the entropy difference

$$\Delta S_{sn} = S_n(T) - S_s(T)$$

and the free energy difference

$$\Delta F_{sn}^{(0)} = F_n(T, 0) - F_s(T, 0) = \frac{H_c^2(T)}{8\pi}.$$

The method of measurements [21], as well as partial results for $H_c(T)$ near T_c [14], have been already published. If, in addition, experimental values for S_i are known for

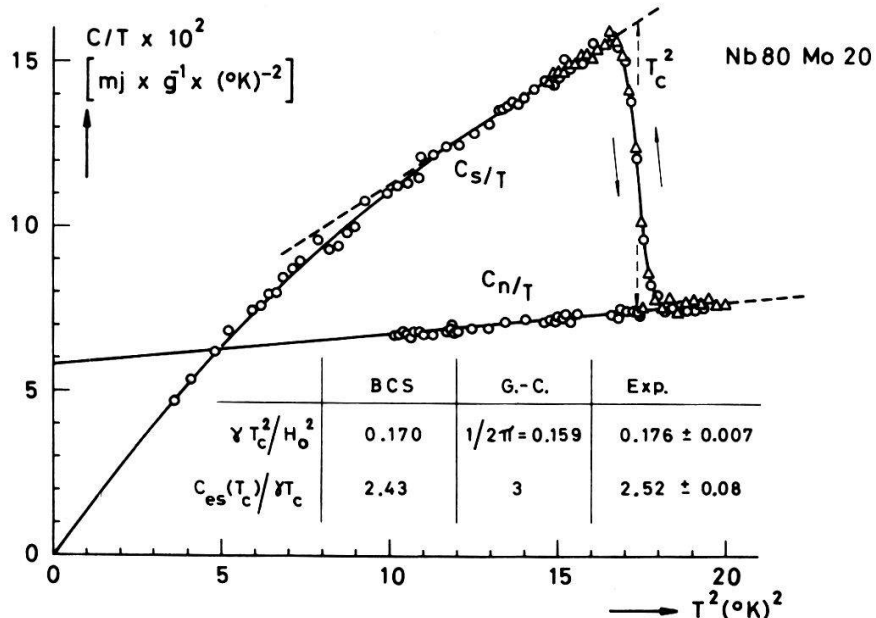


Figure 3

Experimental values for the specific heat in the normal state, C_n , and in the superconducting state, C_s , of the alloy Nb80Mo20. The points marked by circles are obtained in increasing temperature, those marked by triangles in decreasing temperature.

arbitrary fields at different fixed temperatures, the variation of the energy function, $\Delta U_{sn}(T) = \Delta Q_{sn}(T) + \Delta I_{sn}(T)$, may be determined experimentally. The calorific energy ΔQ_{sn} and the magnetic energy ΔI_{sn} are the energies necessary to allow the sample to transform quasistatically from the superconducting to the normal state, but without the requirement that this transition ought to be reversible [22]. The isothermal calorimetric method proposed by Otter and Yntema [22], generalized by Hopkins et al. [23], may then also be used to determine $H_c(T)$.

The results obtained from both methods are compared in Table I. Very good agreement is verified for T larger than 3°K, where $\Delta I_{sn} \ll \Delta Q_{sn}$. The magnetization values used to calculate ΔI_{sn} have been measured in the middle part of the cylindrical sample [14]. They ought to be corrected slightly to take into account end effects due to the finite length of sample. This correction cannot be neglected at lower temperatures, which

Table I
Experimental values for the thermodynamic critical field H_c of the alloy Nb80Mo20 as a function of temperature ($T_c = 4.16^\circ\text{K}$)

$T^\dagger)$ (°K)	$H_c^\ddagger)$ (Oe)	$H_c^\S)$ (Oe)	$\frac{H_c^\S - H_c^\ddagger}{H_c^\ddagger} \parallel$ (%)
4.16	0	0	0
4	47.4	47.2	-0.4
3.75	120.2	120.9	+0.6
3.5	190.9	189.9	-0.5
3.25	257.4	256.4	-0.4
3	320.5	321.4	+0.3
2.75	379.8	383.1	+0.9
2.5	435	441	+1.4
2.25	486	494	+1.7
2	532	542	+2.0
1.5	609	—	—
1	666	—	—
0.5	700	—	—
0	711	—	—

†) Temperature, ‡) results from specific heat measurements, §) results from isothermal calorimetry, ||) comparison of results, in per cent.

explains the slight systematic and increasing discrepancy observed. At very low temperatures, the fields necessary to reach H_{c2} are too large ($\gtrsim 3\text{kOe}$) for our solenoid system.

The parabolic curve, determined by the points [$T = 0$, $H = H_c(0)$] and [$T = T_c$, $H = 0$], is represented by the equation: $h^*(t) = 1 - t^2$, with $t = T/T_c$ as the reduced

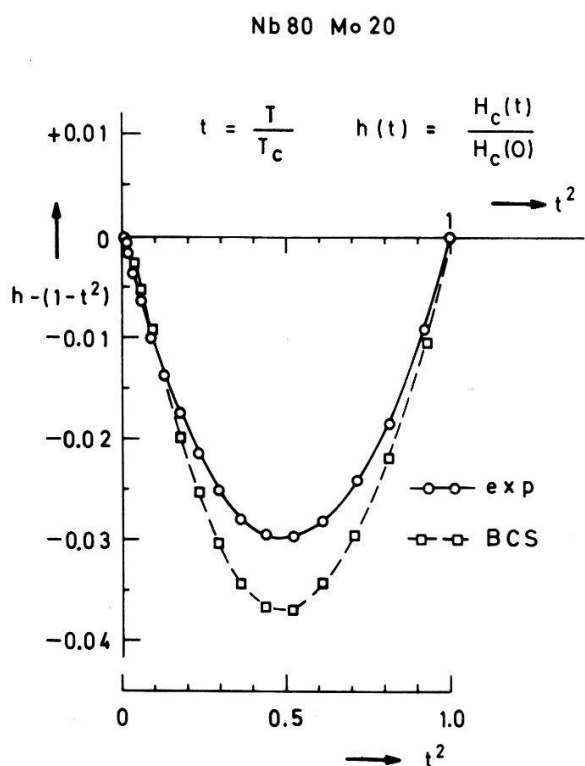


Figure 4
Comparison of experimental results with the theoretical BCS expectations for $H_c(T)$, the thermodynamic critical field, as a function of the reduced temperature.

temperature and $h^*(t) = [H_c(T)/H_c(0)]$ as the reduced field. From the BCS theory [24], the deviation law, $h - h^*$ (h experimental), ought to be universal for weak-coupling superconductors. Experimental values for $(h - h^*)$ at temperatures below T_c are plotted in Figure 4, as well as BCS values calculated by Muehlschlaegel [25]. Good agreement is obtained.

From specific heat measurements, we get experimental values for the following quantities: γ (Sommerfeld constant) = $(5.12 \pm 0.05) \times 10^3$ erg.cm $^{-3} \cdot ^\circ\text{K}^{-1}$; θ (Debye temperature) = $276 \pm 3^\circ\text{K}$; T_c (critical temperature) = $4.160 \pm 0.003^\circ\text{K}$; H_0 (thermodynamic critical field) = $H_c(T = 0^\circ\text{K}) = 711 \pm 5$ Oe. A mean molecular weight of $\bar{M} = 93.5$ and a specific mass of $\rho = 8.93$ g.cm $^{-3}$ have been used for the calculations. Introducing these experimental data into the BCS relation, $T_c = 0.85\theta\exp(-1/NV)$, we get the value, $NV = 0.23$, for the product of the density of states, N , with the electron-electron interaction parameter V . This value is close to the one for tin (0.25), which shows for $H_c(T)$ an analogous temperature behaviour. The experimental values for $[C_{cs}(T_c)]/\gamma T_c = 2.52 \pm 0.08$ and $\gamma T_c^2/H_0 = 0.176 \pm 0.007$ are to be compared with the respective BCS values, 2.43 and 0.170. Finally, the energy gap at 0°K may be estimated from relations derived by several authors, and compared with the BCS value, 3.53:

$$\frac{2\Delta}{kT_c} = \frac{4\pi}{\sqrt{3}} \left[\frac{H_0^2}{8\pi\gamma T_c^2} \right]^{1/2} = 3.45 \pm 0.09 \quad (\text{Ref. [26]})$$

$$\frac{2\Delta}{kT_c} = \frac{2T_c}{H_0} \left(\frac{dH_c}{dT} \right)_{T_c} = 3.67 \pm 0.09 \quad (\text{Ref. [27]})$$

$$\frac{2\Delta}{kT_c} = 2 \left[\frac{C_s(T_c) - C_n(T_c)}{0.27 \cdot \gamma \cdot T_c} \right]^{1/3} = 3.56 \pm 0.04 \quad (\text{Ref. [28]}).$$

All these numerical results confirm in general the BCS predictions.

From magnetic measurements on a number of Nb-Mo alloys with different concentrations, it could be deduced [20] that alloying Nb increases the tendency to weak-coupling behaviour. It is now confirmed that the alloy Nb80Mo20 behaves as a weak-coupling superconductor.

V. Experimental Values for the Free Energy in the Mixed State

1. Experimental determination of $\Delta S(T, B)$ and $\Delta F(T, B)$

The incremental entropy of vortices, S_i , has been measured as a function of H ($0 \ll H < 2$ kOe) for twelve different temperature values T_1, T_2 , and so on, ranging between 1.5°K and 4.11°K (method of measurements, see Ref. [21]). After having determined the constitutive relation $B = B(H, T)$ from reversible magnetization curves [14], S_i values may be plotted as a function of B (Fig. 7). Errors on B , in interpreting the experimental magnetization curves, ought not to exceed 1%. Integrating $S_i(B)$, we get:

$$\Delta S(T, B) = S(T, B) - S_s(T) = \frac{1}{\phi_0} \int_0^B S_i(T, B) dB = \Delta S_{sn} - \frac{1}{\phi_0} \int_B^{H_{c2}} S_i(T, B) dB. \quad (23)$$

At a given temperature, ΔS may thus be obtained for arbitrary B values. The curves at constant B , $\Delta S(T)|_B$, may be drawn through the points $[T_1, \Delta S(T_1, B)]$, $[T_2, \Delta S(T_2, B)]$, etc. (Fig. 9), assuming a continuous behaviour for the slope $\partial(\Delta S)/\partial T|_B$.

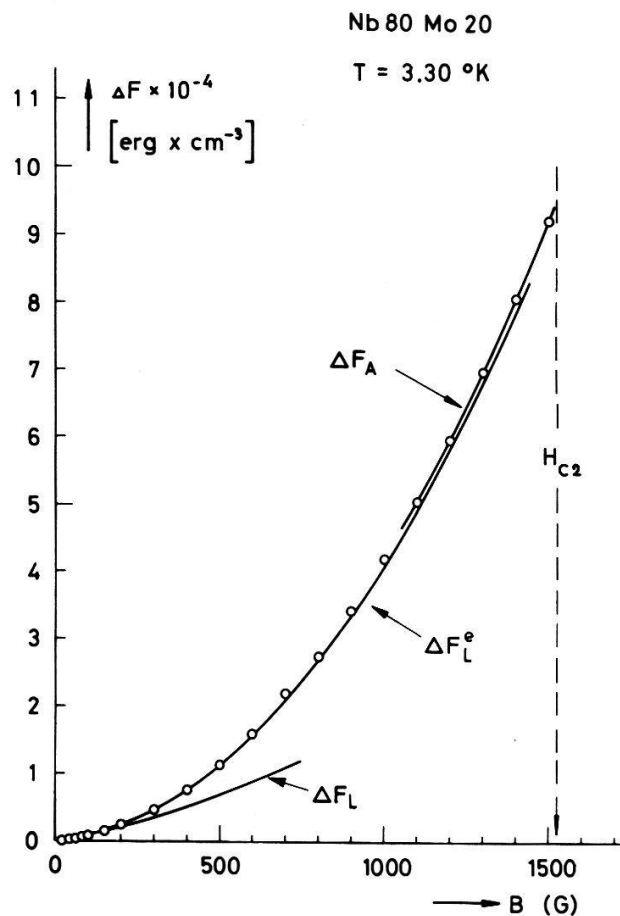


Figure 5

Experimental and theoretical values, in the mixed state, for the free energy difference, $\Delta F = F - F_s$, as a function of the induction B at a given temperature. F is the free energy in the mixed state, F_s the free energy in the superconducting state. The theoretical functions $\Delta F_L = F_L - F_s$, $\Delta F_L^e = F_L^e - F_s$ and $\Delta F_A = F_A - F_s$ are calculated from the free energies in the mixed state according to the London theory, extended London theory and Abrikosov theory as discussed in Section II.

Values of ΔF for arbitrary T , at a given B , may be obtained integrating the curves $\Delta S(T)|_B$:

$$\Delta F(T, B) = F(T, B) - F_s(T, 0) = \Delta F_{sn}(T_{c2}) + \int_T^{T_{c2}} \Delta S(T, B) dT$$

$$\Delta F_{sn}(T_{c2}) = \frac{H_{c2}}{8\pi} (T_{c2}) + \frac{B^2}{8\pi} \quad (24)$$

The temperature T_{c2} is the critical temperature at which the mixed-normal state transition occurs, for a given and constant B .

Such experimental values for ΔF have been plotted in Figure 5, as a function of B , at 3.3°K. The theoretical values for F_L , F_L^e and F_A (generalized Abrikosov free energy) have been drawn as full curves. The agreement is excellent. Surprisingly, the theoretical

energy F_L^e accounts for the behaviour in nearly the whole range of B , although it is not expected that this relation holds for a K of 4 only. Nevertheless, remembering that the value of $B^2/8\pi$ is about 98% of the total energy near H_{c2} , the quantity $[\Delta F - (B^2/8\pi)]$, instead of ΔF , has to be plotted for a detailed comparison.

2. Detailed comparison of the experimental and theoretical values for $S_i(B)$ and $F(B)$: $0^\circ\text{K} \ll T < T_c$

A number of parameters are implicated in the theoretical relations (10), (14) and (17) for free energies, the values of which must be estimated, if not measured or calculated. The experimental values for H_{c2} and γ_2 deduced from specific heat and magnetization measurements [14], are used. Concerning H_{c1} , it has been shown that the observed

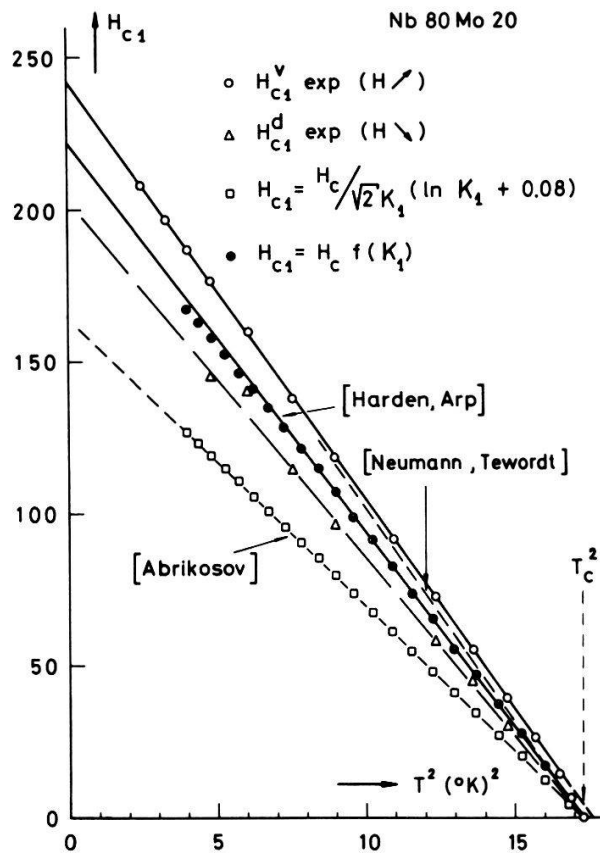


Figure 6

Experimental values for the first critical field determined in increasing field (H_{c1}^v) and decreasing field (H_{c1}^d) from magnetization measurements [14], compared with theoretical values. For the Neumann-Tewordt calculation, see Ref. [30].

first penetration field H_{c1}^v is not the thermodynamic field H_{c1} . Values of H_{c1} have been calculated from the Harden and Arp [29] numerical relation $H_{c1}/H_c = f(K)$, using calorimetric values for H_c and experimental K_1 values (see Fig. 6). A reasonable agreement is thus found with H_{c1} values deduced in interpreting the magnetization curves [14]. $\xi(T)$ and $\lambda(T)$ are calculated by means of the GL relations $\xi(T) = (\phi_0/2\pi H_{c2})^{1/2}$ and $\lambda(T) = K(T)\xi(T)$ (Ref. 18, pp. 26, 27, 46), with $K(T)$ approximated as $K_1(T)$. The values of derivatives are obtained by graphical differentiation of the curves $\lambda(T)$, $\xi(T)$ and $\varphi(T)$ (see Table II).

In Figure 7a-d, the experimental and theoretical values for S_i and $(\Delta F - B^2/8\pi)$ are plotted as a function of the reduced induction B/H_{c2} (H_{c2} for \bar{H}_{c2} , see Section III). The theoretical expression F_L^e for the energy, which was shown to hold approximately in the whole mixed state, depends essentially on the ratios d/λ and λ/ξ , i.e. on B/H_{c2} , since we get from GLAG theory:

$$\frac{B}{H_{c2}} = \left(\frac{4\pi}{\sqrt{3}} \right) \left(\frac{\xi}{d} \right)^2 = \left(\frac{4\pi}{\sqrt{3}K^2} \right) \left(\frac{\lambda}{d} \right)^2.$$

Plotting this quantity on the horizontal axis, a similar behaviour is thus expected, and observed, for different values of temperature.

Table II

Numerical values used for the parameters in the calculation of the London free energy F_L and its extension F_L^e

$T \dagger)$ (°K)	$K(T) \ddagger)$	$\lambda \S)$ (cm)	$\xi \parallel)$ (cm)	$\lambda' = \frac{\partial \lambda}{\partial T}$ [cm.(°K) $^{-1}$]	$\xi' = \frac{\partial \xi}{\partial T}$ [cm.(°K) $^{-1}$]	$\varphi' = \frac{\partial \varphi}{\partial T} \parallel)$ [Oe.(°K) $^{-1}$]	$\psi \parallel)$
4.11	4.10	$8.20 \cdot 10^{-5}$	$2.00 \cdot 10^{-5}$	$63.6 \cdot 10^{-5}$	$15.7 \cdot 10^{-5}$	-77.6	0
4.06	4.12	5.48	1.33	30.0	7.4	-75.8	+0.01
3.96	4.16	3.98	0.96	10.3	2.57	-72.3	+0.02
3.84	4.22	3.18	0.76	4.83	1.22	-68.4	+0.04
3.69	4.28	2.65	0.62	2.52	0.65	-63.7	+0.06
3.51	4.36	2.32	0.53	1.49	0.40	-58.5	+0.08
3.30	4.45	2.06	0.46	1.00	0.27	-53.0	+0.12
3.00	4.57	1.82	0.40	0.59	0.17	-45.0	+0.17

†) Temperature, ‡) GL parameter, §) penetration depth, ||) coherence length, ¶) definition of the functions $\varphi(T)$ and $\psi(T)$, see Section II.

In the lower part of the figures, the theoretical curves are indicated as full curves within the region of validity and as dashed curves outside. The corresponding theoretical curves for S_i may be easily identified in the upper part of the figures.

From the first of the relations (13), a linear, slightly decreasing behaviour with B is predicted at high fields. In the low field region, the theory predicts a minimum for $d \approx 3\lambda$ [relation (16)]. This behaviour has evidently no physical meaning and comparison with theory ought to occur only for $B/H_{c2} < 0.03$. Concerning the intermediate region ($d < \lambda$, $B/H_{c2} > \sim 0.4$), it appears immediately that theory accounts only qualitatively for experimental results, on a detailed and sensitive scale.

Before concluding on the agreement between theory and experience, the two following effects included in S_i measurements have to be discussed:

- The magnetization is measured with detection coils in the central part of the specimen (cylinder with rounded ends), while the measured temperature holds for the whole bulk [14]. Thus, calorimetric measurements are sensitive to penetration of fluxoids, below H_{c1}^v , into the ends of the specimen (end effect) while magnetic measurements are not. Consequently, our S_i measurements cannot be used, unless corrected, for fields H smaller than H_l , with H_l proportional to and about 10% larger than H_{c1}^v . Above H_l , the corrections on measured ΔB values become negligible. This effect is overwhelmed, at high temperatures, by the effect arising from inhomogeneous impurity concentration.

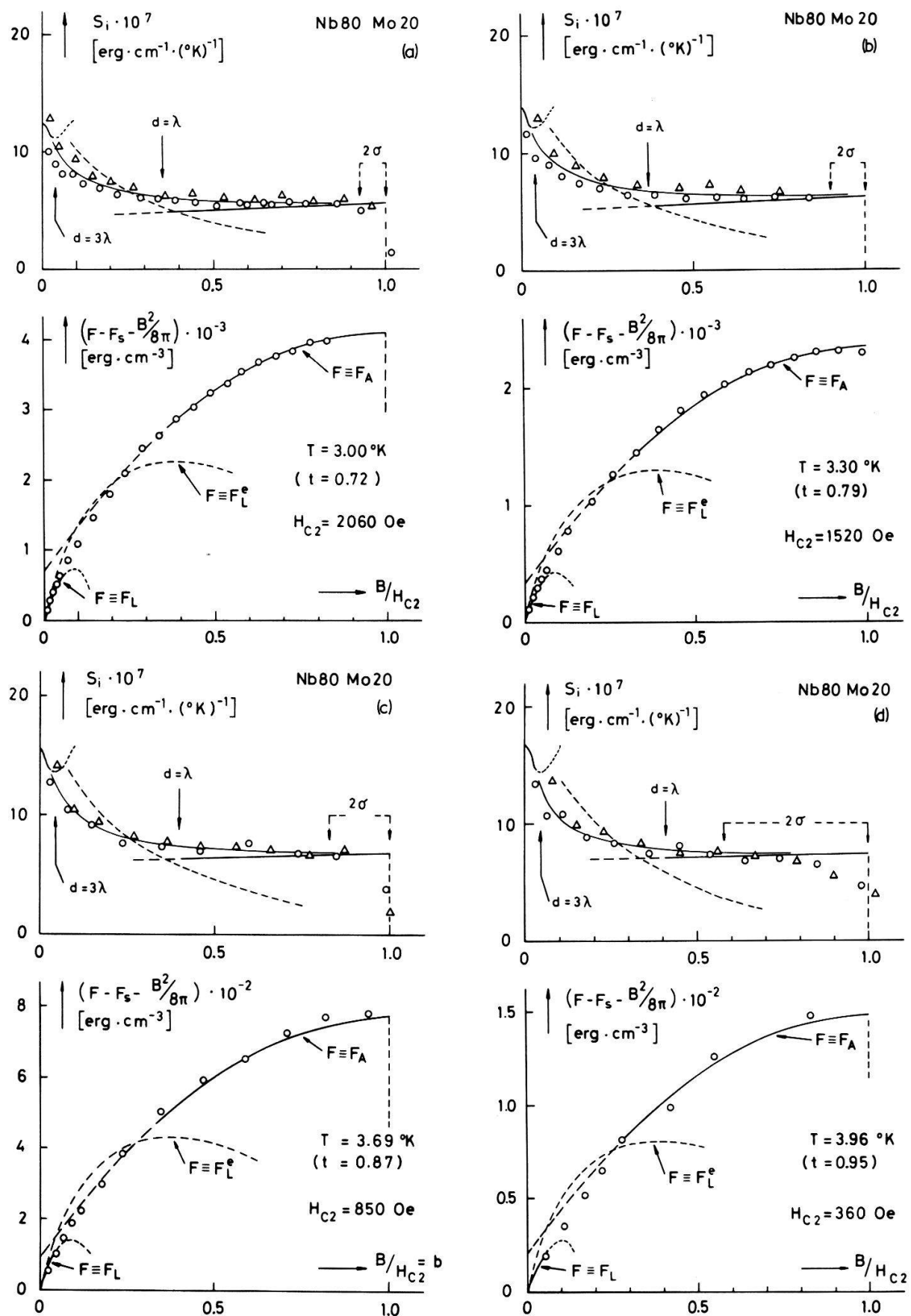


Figure 7a-d

Detailed comparison of experimental and theoretical values for the incremental entropy $S_i(B/H_{c2})$ and the free energy $F(B/H_{c2})$, as a function of the reduced induction, at different temperatures near T_c . Experimental points obtained with increasing field are denoted by circles, those with decreasing field by triangles. The interval 2σ is correlated to the standard deviation of the distribution function N of Figure 2.

ii) A distribution function $N[T_c(\nu)]$, for the impurities inside the specimen, has been analysed in Section III. Let $\delta T_c (= 0.043^\circ\text{K})$ be the standard deviation of this assumed gaussian function. The standard deviation of $N[H_{c2}(\nu)]$ is given by

$$\sigma H_{c2} = \delta T_c \cdot \left(\frac{dH_{c2}}{dT} \right)_{T_c} \approx \text{const.} \approx 80 \text{ Oe.}$$

Experimental points, lying within $1 - 2\sigma < B/H_{c2} < 1$, have to be excluded for comparison with theory, since more than 2% of the bulk is already in the normal state ($\alpha > 0.02$). The same holds for points (not drawn in figures) lying within $0 < (B/H_{c2}) < 2\tau$, with

$$\tau H_{c2} = \delta T_c \left(\frac{dH_{c1}}{dT} \right)_{T_c} \approx \text{const.} \approx 4 \text{ Oe.}$$

On the other hand, within $2\tau < B/H_{c2} < 1 - 2\sigma$, results ought to be the same as if the concentration of impurities would be homogeneous ($\nu \equiv \bar{\nu}$) since S_i is a slowly varying function with B . It can be verified that this region becomes more and more narrow as T goes to T_c .

It is to be noted that the comparison of experimental and theoretical values close to $B \approx 0$ can be done with confidence at low temperatures only (small τ values). For the highest temperature reported here ($T = 3.96^\circ\text{K}$), no experimental point could be used for direct comparison with the theory ($2\tau \approx 0.02$).

Consequently, in the measurable region ($2\tau < B/H_{c2} < 1 - 2\sigma$), an experimental (full) curve has been drawn as the mean curve through the points obtained with increasing field (circles), and decreasing field (triangles). The extrapolation of this curve to $B = 1$ is easy, and gives results in very good agreement with theoretical predictions. Such an agreement was already verified below $T = 4.1^\circ\text{K}$ from specific heat measurements [14]. Close to $B = 0$, the theoretical curve coincides reasonably with the experimental results. Integrating along this so-defined quasi-experimental curve between $B = 0$ and $B = H_{c2}$, values of $\Delta S_{sn}(T)$ are obtained which have been found, within 2%, to be in agreement with values obtained from independent specific heat measurements.

3. Comparison of experimental and theoretical values for $S_i(H_{c2})$, at any temperature

Experimental values for $S_i(H_{c2})$ have been plotted in Figure 8, at thirteen different temperatures, between 1.5°K ($t = 0.36$) and 3.96°K ($t = 0.95$). For $t > 3^\circ\text{K}$ ($t = 0.72$), values are reliable as equilibrium values while for lower temperatures irreversibility increases as temperature decreases. Thus, the results at low temperature are probably too small, because measurements could be made with increasing field only, and not close enough to H_{c2} to get good extrapolated values. Such an observed irreversibility (see for example Fig. 7a) may partially be due to the impulse method of measurements [21].

The theoretical curve 1 has been calculated from the first of relations (13), using experimental values for K_2 and dH_{c2}/dT deduced from magnetization and specific

heat measurements [14]. An excellent agreement with experimental results is found for $t \lesssim 0.7$. On the other hand, there is evidence that the theoretical curve deviates upwards at low temperature, probably because of uncertainties in determining the magnetic parameters, at high fields.

The theoretical curve 2 has been calculated, rewriting the relation (13) as follows,

$$S_i(H_{c2}) = -\frac{\phi_0}{4\pi\gamma_2(T)} \frac{d}{dT} [\sqrt{2}K_1(T) H_c(T)],$$

and using the temperature-dependent $K_1(T)$ and $K_2(T)$ values given by Eilenberger [15], for the experimental $K(T_c)$ value 4.1 of our sample. The field H_c is the BCS field, which has been shown to be practically identical, in our case, with the experimental

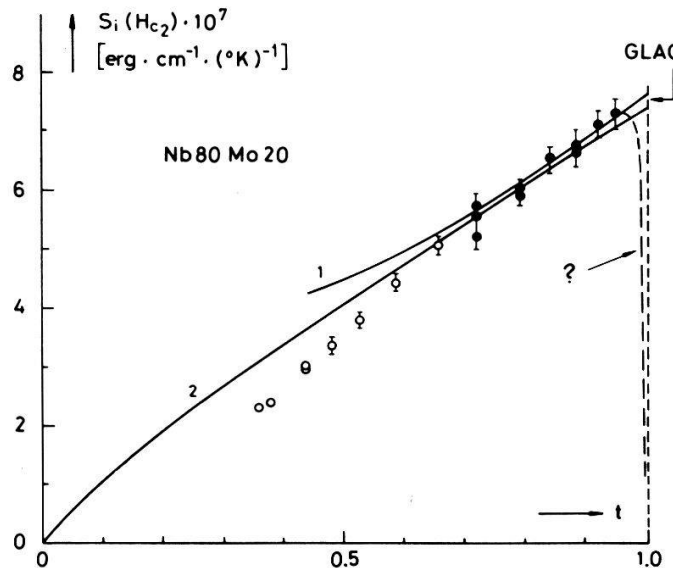


Figure 8

Experimental values for the incremental entropy of vortices S_i , at the mixed-normal state transition, as a function of the reduced temperature t . Full circles represent mean values between results of measurements in increasing and decreasing fields, open circles represent results of measurements in increasing field only. The calculation of theoretical curves 1 and 2 is described in the text. The hypothetical behaviour close to T_c (dashed curve) results from deductions of Section VII.

H_c (Section IV). It is surprising that curve 2 accounts for equilibrium experimental results probably in the whole temperature range, though the theoretical temperature dependence for K_1 and K_2 was found to be too small [14].

The theoretical value for $S_i(0)$ is zero, in agreement with the third principle of thermodynamics. Admitting that the theoretical relation (7) holds at any temperature, this implies that $(dH_{c2}/dT)_{T=0} = 0$, consequently $(dK_1/dT)_{T=0} = 0$, provided that K_2 does not diverge near 0°K. The dashed curve, noted by a question mark, characterizes an eventual behaviour of S_i , close to T_c , resulting from assumptions and deductions developed in Section VII.

VI. Entropy in the Mixed State Close to the Critical Temperature

The curve $\Delta S_{sn}(t) = S_n(T) - S_s(T)$ is a bell-shaped curve, the two branches of which go to zero, the left branch at 0°K and the right branch at T_c . For H_c strictly parabolic, the maximum occurs at $T = T_c/\sqrt{3}$ [31]. In the case of Nb80Mo20 (BCS

superconductor) we get $C_s = C_n$ for $T = 2.21^\circ\text{K}$, instead of $T_c/\sqrt{3} = 2.40^\circ\text{K}$. The part of the right branch of $\Delta S_{sn}(T)$, close to T_c , is shown in Figure 9. Points on this curve are representative for all normal states, at $T \ll T_c$. Points on the horizontal axis ($0 \ll T \ll T_c, \Delta S = 0$) are representative for all pure superconducting states [$T \ll T_c, H \ll H_{c1}(T)$]. In the space between, we find values for the entropy in the mixed state. Points outside are not representative for any state, except those lying on the horizontal axis, for the normal state ($T > T_c$).

From any point on the $\Delta S_{sn}(T)$ curve, a B curve $\Delta S(T)|_B$ (Section V.1), and a H curve, $\Delta S(T)|_H$, may be drawn. All B curves converge to zero at 0°K , while H curves

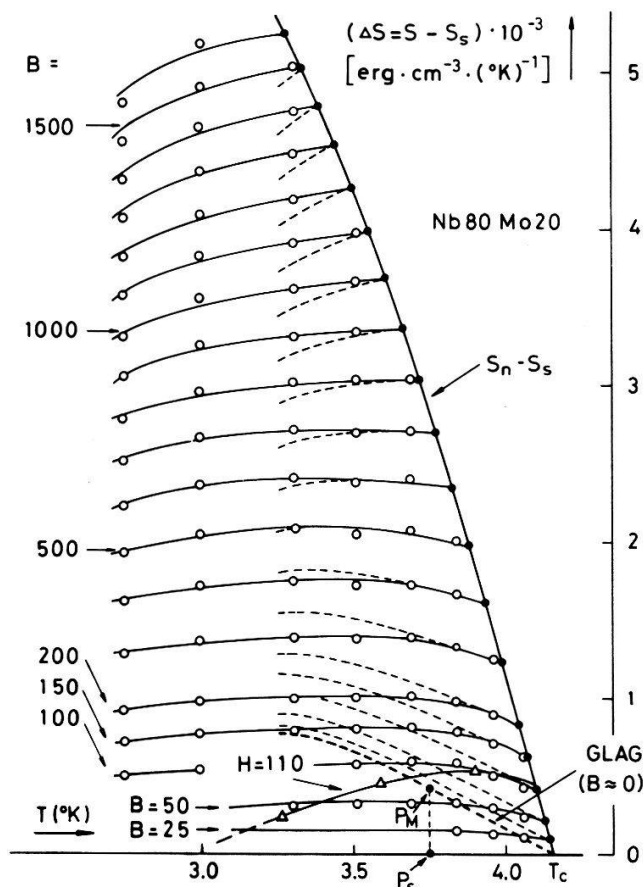


Figure 9

Entropy difference, $\Delta S = S - S_s$, between the superconducting and the mixed-normal state respectively, for the alloy Nb80Mo20 ($K \approx 4$), in the region near T_c . The full curves join the experimental points (circles) with constant induction B . The theoretical curves at constant induction $\Delta S(T)|_B$, calculated by means of relation (12) of Section II, are shown as dashed curves.

reach the horizontal axis for $T > 0^\circ\text{K}$ as long as $H < H_{c1}(0)$. Experimental B curves have been traced for $B = 25, 50, 100, 150, 200, 300$ G, and so on. The uncertainty on the vertical position of an individual experimental point, at a given temperature T , ought not to exceed 2% of $\Delta S_{sn}(T)$ (Section V.2). In an analogous way, we get H curves from suitable integration of specific heat measurements in a constant magnetic field. Only one H curve has been drawn ($H = 110$ Oe) for sake of legibility. The points for which $B = 100$ G, 80 G and 50 G and belonging to this H curve have been indicated as triangles. They ought also to lie on the respective B curves, which was found to be true in general only for points lying not too far away from T_c , because of increasing uncertainties as T decreases.

The theoretical B curves have been drawn as dashed curves. They have been calculated from the first of the relations (12), using a mean $K(T)$ value which is identical to the experimental $K_1(T)$ and $K_2(T)$ for $T > 3.6^\circ\text{K}$. For clarity, the calculation was done within a large temperature range at low B , although the theoretical relation is not expected to hold far away from T_{c2} .

The following remarks should be made:

- a) For $T < 3.6^\circ\text{K}$ ($B > 1000$ G), bad agreement is found between experimental and theoretical curves, even close to T_{c2} . Better agreement would be found using the suitable K_2 parameter for the calculation. However, experimental points are too few and not so reliable at high fields, to draw conclusions.
- b) For $3.6^\circ\text{K} < T < 4.1^\circ\text{K}$ (100 G $< B < 1000$ G), both slopes at T_{c2} are in excellent agreement. Moreover, an optimal agreement is observed for $B = 500$ G, where both curves are identical within a temperature interval as large as 0.6°K .
- c) For $T > 4.1^\circ\text{K}$ ($B < 100$ G), an apparent increasing disagreement is observed as B goes to zero. Indeed, as a result of a natural interpolation of experimental B curves between $T = 4.06^\circ\text{K}$ and T_{c2} , we conclude that the slope $\partial(\Delta S)/\partial T|_B$ is vanishingly small as T_{c2} goes to T_c ($\beta_B^* = 1$). On the other hand, the theory predicts at the limit a finite negative slope (Section II.3).

These results, close to T_c , have evidently to be compared with the anomalous results for C_H , which were observed on the same sample in the same region of field and temperature (Section I).

VII. Discussion

Specific heat results on the Nb80Mo20 sample studied here have been discussed already [14]. The possibility of the occurrence of size and fluctuation effects to explain the anomalous results close to T_c have been briefly examined and found unlikely. Effects from the physical inhomogeneities could not be discarded but were estimated less probable than an effect resulting from a fundamental modification of the vortex structure.

As an example for such a structure, a suggestion was made about the existence close to T_c of a composite of mixed state domains and Meissner domains. This implies in fact the occurrence of an attractive interaction between vortices for large values of the lattice constant. It is to be noted however that such structures have been observed in critical K superconductors with non-zero demagnetizing coefficients only [32]. Simple considerations show that assuming a constant value d_0 of the vortex lattice parameter for $B \gtrsim 100$ G leads to the observed specific heat results, close to T_c . Furthermore, the order of magnitude ($d_0 \approx 0.5 \mu$) is in agreement with values of d_0 measured on critical K superconductors, in low fields and at $T \ll T_c$, by means of decoration technique or neutron diffraction [32, 33]. We now examine what complementary or additional information may be obtained from C_B measurements.

A question which arises in discussing Figure 9, where the results are summarized, is the following: is the flat behaviour observed for curves $\Delta S(T)|_B$, close to $B = 0$, really in contradiction with a negative slope $\partial(\Delta S)/\partial T|_B$ at the limit $T_{c2} \rightarrow T_c$? Indeed, away from T_c , the theoretical curve which has been drawn for $B \approx 0$ cannot be valid. Because of the continuity of the Gibbs energy at a phase transition, the point P_M ought to be identical with P_S , since no finite entropy difference can correspond, at the

transition, to a vanishingly small induction difference, according to the Clapeyron equation:

$$\frac{dH_{c1}}{dT} = 4\pi \frac{S(P_M) - S(P_S)}{B(P_S) - B(P_M)}. \quad (25)$$

Such a continuous behaviour for entropy is quite in agreement with the theoretical expression for the free energy (14), which implies a λ transition at H_{c1} . Consequently, the domain of validity, close to T_{c2} , for the theoretical relation (12) has to become vanishingly small as T_{c2} goes to T_c . This is effectively observed. As our conclusion on the limiting slope, $\partial(\Delta S)/\partial T|_B$ at T_c , results from an interpolation procedure, it may be argued that if sensitive and direct measurements would be possible, such a negative value for the slope could eventually be detected.

Our conclusion however finds a confirmation in the following way. Setting $\partial(\Delta S)/\partial T|_B$ equal to zero in relation (6), we get: $\partial(\Delta S)/\partial T|_H \geq 0$, i.e. $C_H \geq C_S$. This is exactly the result which has been observed for $C_H(H_{c2})$ from direct measurements close to T_c . Both deviations observed for C_H and C_B from independent calorimetric measurements are then in agreement with thermodynamics. Moreover, applying our analysis of Section III to specific heat results in the case of small fields, it is difficult to find a reason for the magnitude of the jump to be changed in the sense observed. For example, errors in extrapolating experimental results to T_{c2} would indeed create a deviation of opposite sign. Nevertheless, these anomalous results ought to be confirmed on other samples. A definitive and irrefutable proof that the effect is not due to imperfect material is of course difficult to give, mainly because of the three following reasons:

- Samples showing a total reversible calorimetric behaviour, near T_c , are difficult to obtain.
- The broadening of the transitions due to inhomogeneities of concentration may be too large for analysis.
- A high power of resolution is required for measurements.

Having noted these restrictions, we draw consequences from the new feature,

$$\lim_{B \approx H_{c2} \rightarrow 0} \frac{\partial(\Delta S)}{\partial T} \Big|_B = 0,$$

or from (22), $\beta_B^* = 1$. Together with the previously established result, $\beta_H^* = 1$, admitted as experimental evidence, we deduce from (6) that $\lim_{H_{c2} \rightarrow 0} S_i(H_{c2}) = 0$, since $\partial B/\partial H|_T$ is always positive in the mixed state. Thus, as for C_B and C_H , S_i would take, at the limit, the value valid in the Meissner state. This behaviour, which is suggested in Figure 8 (decreasing dashed curve close to T_c), cannot be verified from direct S_i measurements, which are not meaningful in this temperature region. The similar behaviour with temperature, implied by the GLAG theory, for curves $S_i(B)$ (Fig. 7), would no longer be found very close to T_c . This is plausible, from a thermodynamic point of view, remarking that a slope $\partial(\Delta S)/\partial T|_B$ uniformly zero for all temperatures, for $B \approx 0$, is the simplest way to satisfy the continuity requirement for the Gibbs energy at H_{c1} , in the case of a second-order phase transition.

If the predictions of the GLAG theory do not hold at T_c , the possibility of a first-order phase transition at H_{c1} may be finally considered. The existence of such a transition is implied by the assumption that an intermediate-mixed state can be found close to H_{c2} , which was proposed to explain the specific heat results. Indeed, if the distance between vortices at H_{c2} does not increase beyond a value d_0 as H_{c2} goes to zero, because of an attractive interaction between vortices, this effect should be even more observable close to H_{c1} within the same temperature range. Unfortunately, this assumption finds little experimental support in our case. The only support for a first-order phase transition at H_{c1} could be found in specific heat results [14] obtained with increasing temperature on both our samples (Nb80Mo20 and Pb98In2), which showed an increase of the height of the peak at the first critical temperature T_{c1} , as T_{c1} goes to T_c . On the other hand, our measurements of $S_i(H)$ cannot contribute to such an interpretation. Even at H_{c2} , where the transition has always been interpreted as undoubtedly second order, a small latent heat could occur without being detected because of spreading due to inhomogeneities of concentration.

As already mentioned in Section I, these last considerations are not compatible with calculations within the frame of the GL theory which are valid for the case of an infinite medium. If these anomalous results near T_c are to be experimentally confirmed, the GL equations ought to be solved in the presence of a surface before concluding on the validity of the GL theory applied to finite samples.

VIII. Conclusions

The comparison of experimental values for S_i , the incremental entropy of vortices, with values deduced from the extended Abrikosov free energy, shows very good agreement at the mixed-normal state phase transition for all temperatures below T_c . Unfortunately, the experimental results are not meaningful close to T_c , in the region of field where an anomaly was expected to occur (see Section I). This is due to effects arising from an inhomogeneous spatial distribution of impurities inside the sample. The real behaviour of S_i close to H_{c2} could be qualitatively and quantitatively explained from an analysis of the alloy concentration fluctuations obtained by means of an electron microprobe x-ray analyser.

Integrating $S_i(B)$, the entropy curves at constant induction $S(T)|_B$ have been obtained and analysed in the whole mixed state close to T_c . They show that the specific heat at constant induction $C_B(H_{c2})$, like the specific heat at constant field $C_H(H_{c2})$ [14], tends to the remarkable limit, $C_S(T_c)$, for $B \gtrsim 100$ G. Both results for C_B and C_H are shown to be in thermodynamic agreement, which does not definitely exclude, however, that this effect could be typical for imperfect material. All type-II superconductors should be concerned and these experimental results ought to be confirmed or weakened by measurements on better samples.

Acknowledgments

The authors thank Dr. F. Rothen for his contribution to theoretical calculations, as well as for useful discussions. J.-M. Suter and D. Robin solved the computing problems. Dr. MacInnes read the manuscript. The Fond National Suisse pour la Recherche Scientifique is acknowledged for financial support.

REFERENCES

- [1] V. L. GINZBURG and L. D. LANDAU, *Zh. Eksperim. i. Teor. Fiz.* **20**, 1064 (1950).
- [2] A. A. ABRIKOSOV, *Zh. Eksperim. i. Teor. Fiz.* **32**, 1442 (1957) [Sov. Phys. JETP **5**, 1174 (1957)].
- [3] L. P. GORKOV, *Zh. Eksperim. i. Teor. Fiz.* **34**, 735 (1958); **36**, 1918 (1959). Sov. Phys. JETP **7**, 505 (1958); **9**, 1364 (1959).
- [4] A. L. FETTER and P. C. HOHENBERG, *Superconductivity*, edited by R. D. PARKS (Marcel Dekker, New York 1969), Chap. 14.
- [5] A. E. JACOBS, *Phys. Rev. B* **4** (9), 3022 (1971).
- [6] P. EHRENFEST, *Commun. Phys. Lab. Univ. Leiden, Suppl. No. 75b*, 8 (1933).
- [7] A. B. PIPPARD, *The Elements of Classical Thermodynamics* (Cambridge University Press, London 1966), Chap. 9.
- [8] E. MÜLLER-HARTMANN, *Phys. Letters* **23** (9), 521 (1966).
- [9] L. KRAMER, *Phys. Letters* **23** (11), 619 (1966).
- [10] L. KRAMER, *Phys. Rev. B* **3** (11), 3821 (1971).
- [11] P. G. DE GENNES, *Superconductivity of Metals and Alloys* (Benjamin, New York 1966), Chap. 3.
- [12] A. E. JACOBS, *J. Low Temp. Phys.* **10** (1/2), 137 (1973).
- [13] B. SERIN, *Superconductivity*, edited by R. D. PARKS (Marcel Dekker, New York 1969), Chap. 15.
- [14] R. EHRAT and L. RINDERER, *J. Low Temp. Phys.* **7** (5/6), 533 (1972).
- [15] G. EILENBERGER, *Phys. Rev.* **153**, 584 (1967).
- [16] G. N. WATSON, *A Treatise on the Theory of Bessel Functions* (2nd ed.) (Cambridge University Press, London 1958), Chap. 3, p. 77.
- [17] M. J. STEPHEN, *Phys. Rev. Letters* **16** (18), 801 (1966).
- [18] D. SAINT-JAMES, E. J. THOMAS and G. SARMA, *Type-II Superconductivity* (Pergamon Press, 1969), Chap. 3.
- [19] R. R. KAKE, *Phys. Rev.* **166** (2), 471 (1968).
- [20] R. A. FRENCH and J. LOWELL, *Phys. Rev.* **173** (2), 504 (1968).
- [21] R. EHRAT and L. RINDERER, *J. Appl. Math. Phys. (ZAMP)* **24** (2), 225 (1973).
- [22] F. A. OTTER, Jr., and G. B. INTEMA, *Proc. Low Temp. Cal. Conf. Ann. Acad. Sc. Fenniae*, edited by O. V. LOUNASMAA (Helsinki, 1966), pp. 98–103.
- [23] D. C. HOPKINS, R. R. RICE, J. M. CARTER and J. D. HAYES, *Phys. Rev.* **183** (2), 516 (1969).
- [24] J. BARDEEN, L. N. COOPER and J. R. SCHRIEFFER, *Phys. Rev.* **108**, 1175 (1957).
- [25] B. MÜHLSCHLEGE, *Z. Physik.* **155**, 313 (1959).
- [26] B. B. GOODMAN, *Compt. Rend. Acad. Sci.* **246**, 3031 (1958).
- [27] A. M. TOXEN, *Phys. Rev. Letters* **15** (10), 462 (1965).
- [28] T. P. SHEAHEN, *Phys. Rev.* **149**, 370 (1966).
- [29] J. L. HARDEN and V. ARP, *Cryogenics* **3**, 105 (1963).
- [30] L. NEUMANN and L. TEWORDT, *Z. Physik.* **189**, 55 (1966).
- [31] D. SCHOENBERG, *Superconductivity* (Cambridge University Press, 1965), Chap. III.
- [32] U. KRÄGELOH, *Phys. Stat. Sol.* **42**, 559 (1970).
- [33] J. AUER and H. ULLMAIER, EPS Conf., Florence (1971).